Disruption of hierarchical predictive coding during sleep

Melanie Strauss[a,b,1], Jacobo D. Sitt[a,b,c], Jean-Remi King[a,b,c], Maxime Elbaz[d,e], Leila Azizi[a,b], Marco Buiatti[a,b], Lionel Naccache[c], Virginie van Wassenhove[a,b], and Stanislas Dehaene[a,b,f,g,1]

[a]Cognitive Neuroimaging Unit, Institut National de la Santé et de la Recherche Médicale, U992, F-91191 Gif/Yvette, France; [b]NeuroSpin Center, Institute of BioImaging, Commissariat à l'Energie Atomique, F-91191 Gif/Yvette, France; [c]Institut du Cerveau et de la Moelle Épinière Research Center, Institut National de la Santé et de la Recherche Médicale, U975 Paris, France; [d]Centre du sommeil et de la vigilance, Hôpital de l'Hôtel Dieu, Assistance Publique - Hôpitaux de Paris, F-75004 Paris, France; [e]Equipe Vigilance Fatigue Sommeil, Université Paris-Descartes, 75006 Paris, France; [f]Department of Life Sciences, Université Paris 11, 91400 Orsay, France; and [g]Chair of Experimental Cognitive Psychology, Collège de France, F-75005 Paris, France

Contributed by Stanislas Dehaene, February 5, 2015 (sent for review October 24, 2014; reviewed by Jan Born, Karl J. Friston, and Yuval Nir)

When presented with an auditory sequence, the brain acts as a predictive-coding device that extracts regularities in the transition probabilities between sounds and detects unexpected deviations from these regularities. Does such prediction require conscious vigilance, or does it continue to unfold automatically in the sleeping brain? The mismatch negativity and P300 components of the auditory event-related potential, reflecting two steps of auditory novelty detection, have been inconsistently observed in the various sleep stages. To clarify whether these steps remain during sleep, we recorded simultaneous electroencephalographic and magnetoencephalographic signals during wakefulness and during sleep in normal subjects listening to a hierarchical auditory paradigm including short-term (local) and long-term (global) regularities. The global response, reflected in the P300, vanished during sleep, in line with the hypothesis that it is a correlate of high-level conscious error detection. The local mismatch response remained across all sleep stages (N1, N2, and REM sleep), but with an incomplete structure; compared with wakefulness, a specific peak reflecting prediction error vanished during sleep. Those results indicate that sleep leaves initial auditory processing and passive sensory response adaptation intact, but specifically disrupts both short-term and long-term auditory predictive coding.

mismatch response | prediction | magnetoencephalography | MMN | P300

Sleep is considered a state of unconsciousness of the environment in which behavioral responses to external stimuli are drastically reduced (1); however, the depth at which sensory information is processed during sleep, and the precise stage at which processing is disrupted, remain uncertain. According to an early theory of the reduced responsiveness to external stimuli during sleep, the thalamic-gating hypothesis (2), tonic and synchronous thalamic activity during sleep would disrupt the information transmission from the sensory periphery to the cortex. Alternatively, it has been proposed that sleep may induce a loss of integration at a late stage of cortical processing (3–5). Indeed, preserved activation of primary sensory cortices has been reported in electrophysiological studies in animals (6–9) and in neuroimaging studies in humans (10–12). Furthermore, stimuli that have behavioral relevance, such as hearing one's name, may induce a broad spread of activation into higher cortical areas (10) and evoke late scalp event-related potentials (ERPs) (13).

In addition to relevance, novelty also may be a significant factor modulating the propagation of auditory signals during sleep. In the awake state, presenting a novel deviant sound in a sequence of repeated standard ones, the so-called "oddball" paradigm, elicits a series of novelty-related ERPs. The mismatch negativity (MMN) is a frontocentral negative component peaking at around 100–250 ms after deviant tones (14) that arises from auditory areas (15). The P3b, or P300, is a slower, sustained posterior positivity elicited at around 300 ms (16) thought to arise from recurrent interactions in a broad set of interconnected areas, including frontoparietal cortices (17). These two potentials are interpreted as neural correlates of two different hierarchical stages in the process of novelty detection.

According to the predictive coding hypothesis (18), the laminar organization of the cortex enables the formation of internal models of increasing degrees of abstraction at successive levels of the cortical hierarchy. Each model extracts regularities from its bottom-up sensory inputs at a given time scale, and uses these regularities to generate top-down predictions, which are compared with subsequent inputs. Thus, a sound that violates a learned regularity will generate an error signal, which can be used to readjust the model.

Within this framework, the P300 is considered a high-level prediction error signal associated with conscious novelty detection, which is strongly reduced in various nonconscious conditions, such as coma and anesthesia (17, 19–21), whereas the MMN is considered a lower-level preattentive prediction error signal (22–26) that may be generated nonconsciously (15). In fact, two distinct mechanisms are involved during the MMN time window: an active predictive mechanism (MMN proper) and a passive habituation phenomenon known as stimulus-specific adaptation (SSA). SSA follows the repetition of a sound and leads to reduced neural responses. It is theorized that when a rare sound occurs, the activation of a set of nonadapted "fresh

Significance

Sleeping disrupts the conscious awareness of external sounds. We investigated the stage of processing at which this disruption occurs. In the awake brain, when a regular sequence of sounds is presented, a hierarchy of brain areas uses the available regularities to predict forthcoming sounds and to respond with a series of "prediction error" signals when these predictions are violated. Using simultaneous recordings of electroencephalography and magnetoencephalography signals, we discovered that both short-term and long-term brain responses to auditory prediction errors are disrupted during non-rapid eye movement and rapid eye movement sleep; however, the brain still exhibits detectable auditory responses and a capacity to habituate to frequently repeated sounds. Thus, sleep appears to selectively affect the brain's prediction and error detection systems.

Author contributions: M.S., J.D.S., L.N., and S.D. designed research; M.S. performed research; J.-R.K., L.A., M.B., and V.v.W. contributed new reagents/analytic tools; M.S., M.E., and S.D. analyzed data; and M.S., J.D.S., J.-R.K., and S.D. wrote the paper.

Reviewers: J.B., University of Tuebingen; K.J.F., University College London; and Y.N., Tel Aviv University.

The authors declare no conflict of interest.

[1]To whom correspondence may be addressed. Email: strauss.mel@gmail.com or stanislas.dehaene@cea.fr.

This article contains supporting information online at www.pnas.org/lookup/suppl/doi:10.1073/pnas.1501026112/-/DCSupplemental.

afferents" generates recovery of the original neural response. Inasmuch as SSA reduces the impact of redundant sensory inputs, it might be considered a primitive predictive device, yet one that rests only on neurotransmission mechanisms local to each neuron (27). It was initially thought that passive SSA may account for the MMN (28, 29), but there is now evidence that the latter involves active predictive coding mechanisms (22–26). To summarize, at least three successive brain responses to novelty exist: recovery from sensory adaptation, MMN in the proper sense, and P300.

The present study aimed to clarify whether the nonconscious sleeping brain remains able to detect auditory novelty, and whether predictive coding and habituation mechanisms continue to operate during sleep. Previous electroencephalography (EEG) experiments searching for MMN and P300 responses during sleep have yielded partially contradictory results (30–32), in part because EEG measures were affected by uncontrolled noise arising from sleep signals and EEG artifacts. Moreover, the classical oddball paradigm used in these studies did not clearly dissociate the various hierarchical levels of novelty detection. In this paradigm, the late P300 component (P3b) may be confounded with another lower-level positive component (P3a) that arises automatically shortly after the MMN (33). Furthermore, many oddball paradigms fail to dissociate prediction from adaptation; the deviant sound exhibits both a low absolute frequency and a low transition probability relative to preceding sounds, leading to violations of both adaptation and prediction.

Here we obtained simultaneous EEG and magnetoencephalography (MEG) recordings during wakefulness and during nonrapid eye movement (NREM) and rapid eye movement (REM) sleep, thereby affording better signal-to-noise ratio and spatial resolution than previous EEG recordings. In experiment 1, to probe the hierarchy of novelty detection processes, we used the local/global paradigm, a variant of the oddball paradigm that disentangles the MMN and the P300 (19). This paradigm comprises two nested levels of temporal regularities, a short time scale structure, termed "local," and a longer time scale structure, termed "global" (Fig. 1). Violations of local regularities elicit MMN/P3a responses, whereas violations of global regularities elicit a P300 response (19, 25).

In patients with disorders of consciousness, this paradigm successfully dissociated conscious from nonconscious states based on the presence or absence of the P300 after global violations, whereas the MMN remained present under nonconscious conditions (19, 33–35). Using the local-global paradigm during sleep should dissociate high-level predictive coding reflected in the P300 from lower-level prediction or adaptation effects reflected in the MMN. To further disentangle prediction from adaptation, in experiment 2 we used an aBaBa paradigm in which the two mechanisms work in opposite ways: predictive coding induces a mismatch response (MMR) to rare stimulus repetitions (aa), whereas sensory adaptation induces an enhanced response to stimulus alternations (aB) (26, 36).

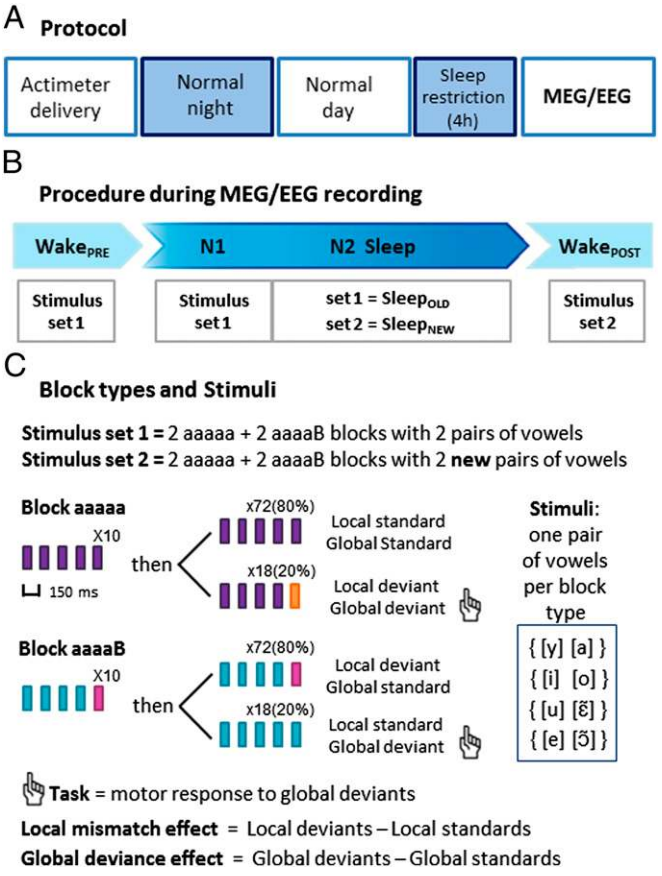

Fig. 1. Experimental protocol. (*A*) Sleeping in the MEG was facilitated by sleep restriction during the previous night, as controlled by actimetry. (*B*) Recordings were obtained during three sessions with auditory stimuli: before (Wake$_{PRE}$), during (Sleep), and after the nap (Wake$_{POST}$). The goal was to evaluate whether the brain reacts to local and global novelty during sleep, and to test whether those effects depend on having previously heard the stimuli in the waking state or whether they can be acquired during sleep. A first set of four blocks was presented during Wake$_{PRE}$ (stimulus set 1), then again while subjects fell asleep (N1 sleep). When subjects reached stage 2 (N2 sleep), in addition to stimulus set 1, a set of 4 new blocks with new stimuli was introduced (stimulus set 2). The corresponding datasets were called Sleep$_{OLD}$ and Sleep$_{NEW}$. Finally, stimulus set 2 was again presented during Wake$_{POST}$. (*C*) Sequences with five identical vowels were termed "local standards", and sequences in which the fifth vowel was different (thus generating a local mismatch effect) were termed "local deviants." In each block, one sequence (local standard in aaaaa blocks or local deviant in aaaaB blocks) was selected and was repeated 10 times then on 80% of the trials, thus establishing a "global standard." The other sequences (respectively local deviant or local standard), termed "global deviant," were presented on the remaining 20% of trials (thus generating a global deviance effect). Subjects were asked to press a button to global deviants in half of the blocks during Wake$_{PRE}$ and Wake$_{POST}$, and whenever they were aware of them during the Sleep session.

Results

In experiment 1, MEG and EEG data were collected before sleep (Wake$_{PRE}$), during a morning nap (N1, N2, and REM sleep stages), and after awakening (Wake$_{POST}$). During N1 sleep, as subjects fell asleep, they still occasionally responded to global deviants, allowing us to retrospectively split the data into N1-responsive and N1-nonresponsive states. The total number of subjects in each sleep stage varied depending on the number of subjects who reached each stage and on the quality of their data (*Materials and Methods*).

Local Effect: Disruption of the MMR During Sleep. Violations of short-term regularities were analyzed by comparing responses to local deviant and local standard sequences, a contrast termed the local effect (Fig. 1). Using sensor-level statistics, a significant local effect was found across all analyzed states of vigilance, from wakefulness to N2 and REM sleep (Fig. 2*A*). However, the brain response to deviant tones was deeply modified in sleep compared with wakefulness.

During the Wake$_{PRE}$ session, local deviants elicited an MMR over temporal MEG sensors, characterized by three successive steps of auditory processing (Fig. 2*C*): an early deflection (left temporal cluster, 48–100 ms, $P < 0.05$), an intermediate effect of reversed polarity peaking at around 150 ms (120–176 ms, $P < 0.01$), and a late effect spreading from temporal areas toward anterior areas (left temporal-anterior cluster: 240–498 ms, $P < 0.001$). On EEG (Fig. 2*D*), the local effect led to a characteristic MMN:

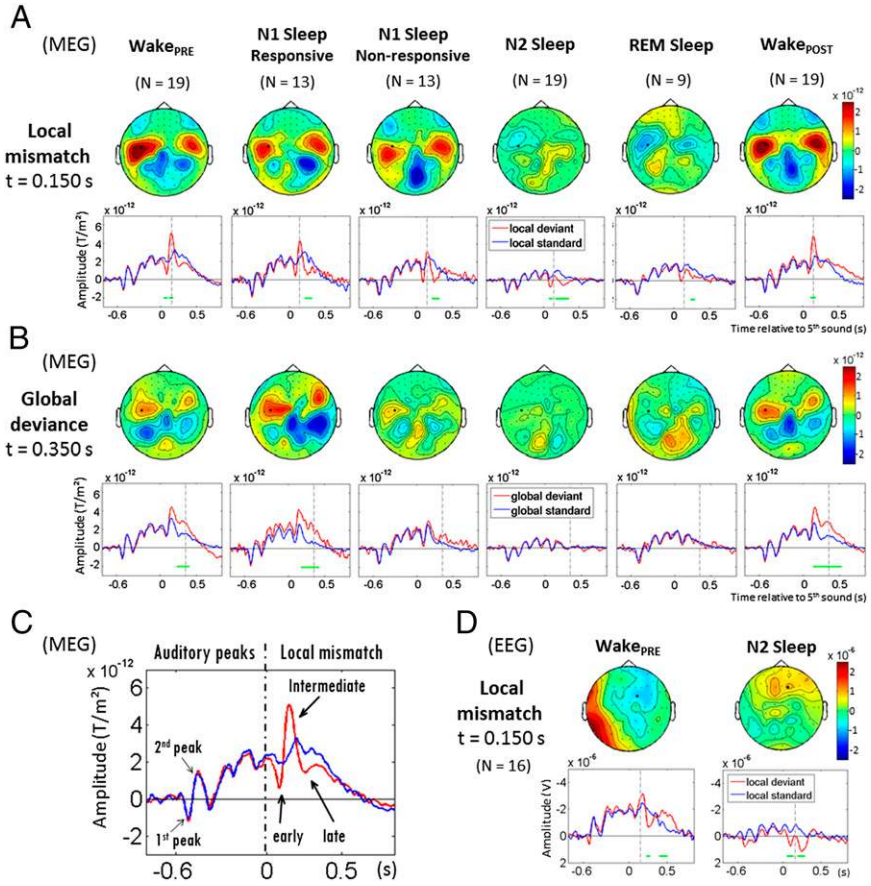

Fig. 2. Event-related responses to local and global novelty as a function of vigilance states. (*A*) Local MMR in MEG. Topographies of the local effect (local standards - local deviants) are shown at $t = 150$ms after the fifth sound. aERFs are shown for local standard and local deviant sequences at one left temporal MEG sensor (black dot, same sensor across states). Cluster-based significant effects ($P < 0.05$, corrected) at this sensor in a 48- to 498-ms time window are represented by green lines. The local mismatch effect is partially preserved across all sleep stages, yet its sharpest central peak, present during wakefulness, vanishes progressively during sleep. (*B*) Global deviance response in MEG. Topographies of the global deviance effect (global deviants - global standards) are shown at $t = 350$ ms after the fifth sound. aERFs are shown for global standard and global deviant sequences at the same left temporal MEG sensor (black dot). Significant effects at this sensor in a 50- to 700-ms time window are shown (green lines). The global effect (P300) is found when subjects are awake, both in Wake$_{PRE}$ and Wake$_{POST}$. It remains present during N1-Sleep when subjects are behaviorally responsive, but disappears as soon as subjects become unresponsive and in all sleep stages. (*C*) Visualization of the first MEG auditory evoked peaks and decomposition of the MEG local mismatch effect into three components during wakefulness (Wake$_{PRE}$): the early effect before 100 ms, the intermediate effect of inverse polarity around 150 ms, and the late effect after 200 ms. (*D*) Local mismatch in EEG, during Wake$_{PRE}$ and N2-Sleep. Topographies are shown at 150 ms. The MMN at 150 ms in Wake$_{PRE}$, contemporaneous of the MEG intermediate effect, vanishes during sleep.

a negative deflection at the vertex at around 150 ms associated with a polarity inversion at the mastoids (128–176 ms, $P < 0.05$), followed by a positivity over frontocentral areas later turning into a broad centroparietal positivity, compatible with P3a/P3b waves (224–448 ms, $P < 10^{-4}$). Only the early effect (before 100 ms) failed to be detected on EEG during wakefulness, despite the significant early deflection visible on MEG. Considering the better signal-to-noise ratio for MEG compared with EEG and for better readability, the following results and statistical analyses are reported only for MEG data (type 2 planar gradiometers; *SI Materials and Methods*). Results for all types of sensors are shown in Fig. S1 and Fig. S2.

During sleep, the early MMR was observed in all sleep stages, but reached significance only in N2 sleep (Sleep$_{(OLD+NEW)}$: 76–128 ms, $P < 0.05$), where its amplitude was slightly larger than in the other sleep stages (Table S1). Crucially, the intermediate effect was missing; its amplitude decreased progressively with the depth of sleep, failing to reach significance from N1-responsive sleep (Fig. 2 *A* and *D*) and creating a significant difference from the wake period (Table S2). The late effect was found in all sleep stages, however (N1-responsive and -nonresponsive: 220–348 ms, $P < 0.01$; N2: 136–356 ms, $P < 0.001$; REM: 236–296 ms, $P < 0.05$), with no differences in amplitude (Table S3).

During wakefulness in the Wake$_{POST}$ session, the MMR recovered virtually the same shape as before sleep (Fig. 2*A*). The early effect failed to reach significance, but the intermediate effect recovered over temporal sensors (left temporal cluster: 116–184 ms, $P < 0.05$), and the late effect was significantly detected over the right temporal-anterior sensors (216–324 ms, $P < 0.05$). When comparing Wake$_{PRE}$ and Wake$_{POST}$, activations differed only during the late time window over the right temporal region, where they were slightly stronger for Wake$_{POST}$ (216–332 ms, $P < 0.05$). Given such minimal differences, we grouped Wake$_{PRE}$ and Wake$_{POST}$ conditions in subsequent figures and analyses.

To test the acquisition of new regularities during sleep, new vowel sequences were introduced during N2 sleep (N2-Sleep$_{NEW}$), along with sequences already heard during wakefulness (N2-Sleep$_{OLD}$). The early effect was not detected by cluster analysis for Sleep$_{OLD}$ and Sleep$_{NEW}$ data separately; however, its amplitude was significantly larger for Sleep$_{NEW}$ than for Sleep$_{OLD}$ stimuli when comparing them with a paired Wilcoxon signed-rank test (Table S1). No intermediate effect was found in either

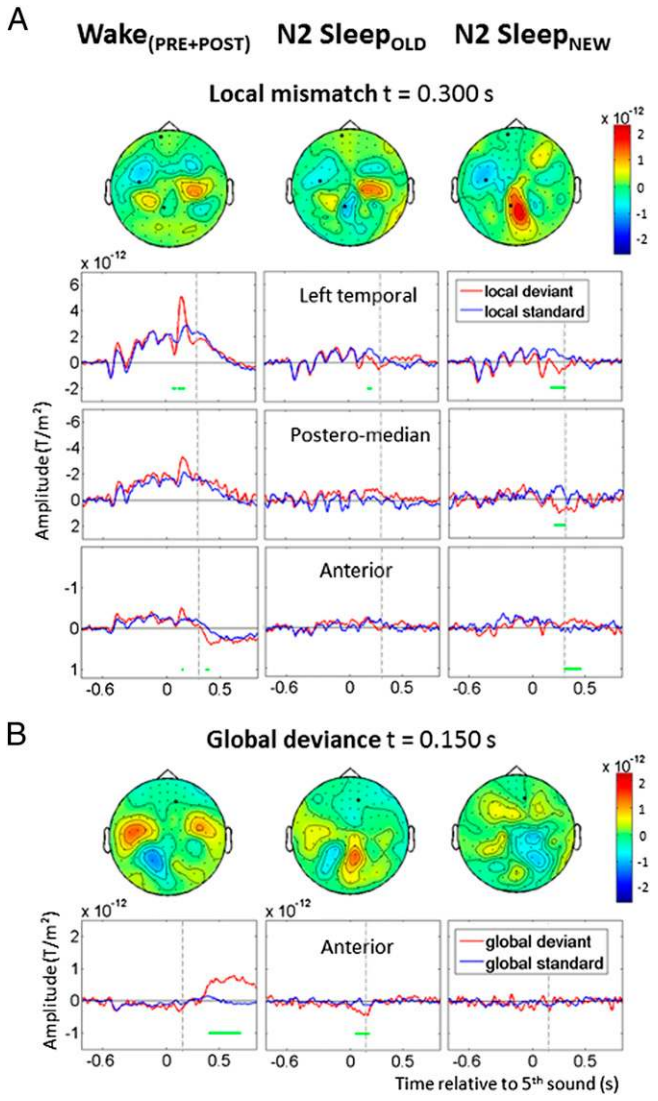

Fig. 3. Effects of previous exposure to sound sequences on the responses to local and global novelty. Each column presents the data from a specific state of vigilance and stimulus set: $Wake_{(PRE+POST)}$ (*Left*), $N2\text{-}Sleep_{OLD}$ (*Center*), and $N2\text{-}Sleep_{NEW}$ (*Right*). (*A*) Local mismatch effect over left temporal, posteromedian, and anterior MEG sensors. Cluster-based significant effects ($P < 0.05$) are represented by green lines. Topographies are shown at 300 ms, when activations between $Sleep_{OLD}$ and $Sleep_{NEW}$ differ significantly. In $Wake_{(PRE+POST)}$, the early and intermediate effects are visible in the left temporal region ($P < 0.01$), whereas the late effect reaches significance only in more anterior areas. In $Sleep_{OLD}$, the significant mismatch effect is limited to a transient late effect over temporal regions ($P < 0.05$). In $Sleep_{NEW}$, when new vowels are introduced during sleep, the late novelty response is enhanced and spreads over posteromedian ($P < 0.01$) and anterior areas ($P < 0.01$). (*B*) Global effect over anterior MEG sensors. Topographies are shown at 150 ms, when activations between $Sleep_{OLD}$ and $Sleep_{NEW}$ differ significantly. In $Wake_{(PRE+POST)}$, the effect over anterior sensors is large and sustained after 400 ms ($P < 0.01$). In $Sleep_{OLD}$, with sequences heard previously during wakefulness, an early transient effect is seen ($P < 0.01$). No global effect is seen for $Sleep_{NEW}$.

condition (Fig. 3*A*). In $N2\text{-}Sleep_{OLD}$, the late effect was detected over left temporal sensors from 176 to 220 ms ($P < 0.05$). In $N2\text{-}Sleep_{NEW}$, the late effect was also detected over left temporal sensors (176–320 ms, $P < 0.05$), with a slightly different topography spreading over posteromedian sensors (92–312 ms, $P < 0.01$) and then anterior sensors (300–406 ms, $P < 0.01$). The direct comparison of $Sleep_{OLD}$ and $Sleep_{NEW}$ stimuli in cluster analysis revealed a significant interaction in the posteromedian region (88–308 ms, $P < 0.05$).

Distributed cortical sources for these effects were computed in $Wake_{(PRE+POST)}$, $N2\text{-}Sleep_{OLD}$, and $N2\text{-}Sleep_{NEW}$ conditions (Fig. 4, *Left*). In all conditions, the early local effect was bilateral and localized in the vicinity of auditory cortices (Wake: maximum at 84 ms, MNI coordinates: −56 −16 13; $Sleep_{OLD}$: maximum at 104 ms, MNI: −49 −16 15; $N2\text{-}Sleep_{NEW}$: maximum at 104 ms, MNI: −47 −36 12). The intermediate effect was visible only during Wake, however. This effect was characterized by strong activations in auditory cortices (maximum at 148 ms; MNI: −52 −36 15) alongside a larger network including inferior frontal gyrus, left parahippocampus, and precuneus. During the late effect, activations during Wake remained sustained in periauditory areas (maximum at 252 ms; MNI: 44 −32 18) and also expanded into broader associative areas (posterior and superior cingulate, insula, parietal lobe, and middle frontal gyrus) (Fig. 4). During sleep, only a subset of these areas remained responsive, at much lower levels, at the time of the late effect ($Sleep_{OLD}$: superior temporal and supramarginalis gyri, right insula, parietal lobe, posterior superior frontal gyrus, and superior cingulate; $Sleep_{NEW}$: bilateral superior temporal and supramarginal gyri and right superior cingulate). Compared with $Sleep_{OLD}$ and Wake, $Sleep_{NEW}$ led to additional late activations in the precuneus (maximum at 240 ms; MNI: 20 −57 23).

We further assessed the similarity of the local novelty response during wakefulness and during sleep using multivariate classification. Within each subject, we trained a decoder to classify each trial as local standard or local deviant at each time point, using the $Wake_{PRE}$ data for training and then testing for generalization to other states of vigilance. This method increases the signal-to-noise ratio, takes into account interindividual variability, and provides a stringent test of the similarities of brain activity patterns across conditions, even in the presence of time delays (37, 38).

The local classifier trained and tested within the $Wake_{PRE}$ session achieved significant decoding scores from 76 to 620 ms ($P < 0.05$), covering early, intermediate, and late MMR effects (Fig. 5*A*, *Left*). The same classifier also generalized fully to the $Wake_{POST}$ session, with results virtually identical to those for $Wake_{PRE}$ (Fig. 5*A*, *Left*). However, when tested on N2-Sleep, the classifier generalized only during the early and late effects (76–100 ms and 212–588 ms, $P < 0.05$). Strikingly, the ∼150-ms peak during which excellent decoding was achieved for Wake data [area under the curve (AUC) ∼0.80] did not generalize at all to sleep (AUC not significantly different from 0.5). Comparing the generalization scores from $Wake_{PRE}$ to Sleep and from $Wake_{PRE}$ to $Wake_{POST}$ confirmed a significant difference from 116 to 484 ms ($P < 0.05$, Wilcoxon signed-rank test). This difference was not related to the absence of novelty response during sleep in the intermediate time period, because when the classifier was trained and tested within the $N2\text{-}Sleep_{(OLD+NEW)}$ dataset (Fig. 5*C*, *Left*), it performed successfully better than chance from 108 to 172 ms ($P < 0.05$). These results indicate that the nature and topography of the novelty response during the intermediate time window in wakefulness differ from those observed during sleep, such that no generalization is possible from one to the other. Similar results were obtained when computing the full temporal generalization matrix (Fig. S3), and also when analyzing the $N2\text{-}Sleep_{OLD}$ and $N2\text{-}Sleep_{NEW}$ trials separately (Fig. 5*B*, *Left*).

Global Effect: Loss of the P300 During Sleep. We next investigated the response to global novelty, that is, the difference between rare and frequent sequences of five sounds. During wakefulness ($Wake_{PRE}$ and $Wake_{POST}$, global deviants were followed by sustained activations, starting over temporal sensors and then spreading toward anterior regions (left anterior temporal cluster, $Wake_{PRE}$: 232–700 ms, $P < 10^{-4}$; $Wake_{POST}$: 144–700 ms, $P < 10^{-4}$) (Fig. 2*B*). Similarly, EEG recordings revealed a posterior positivity

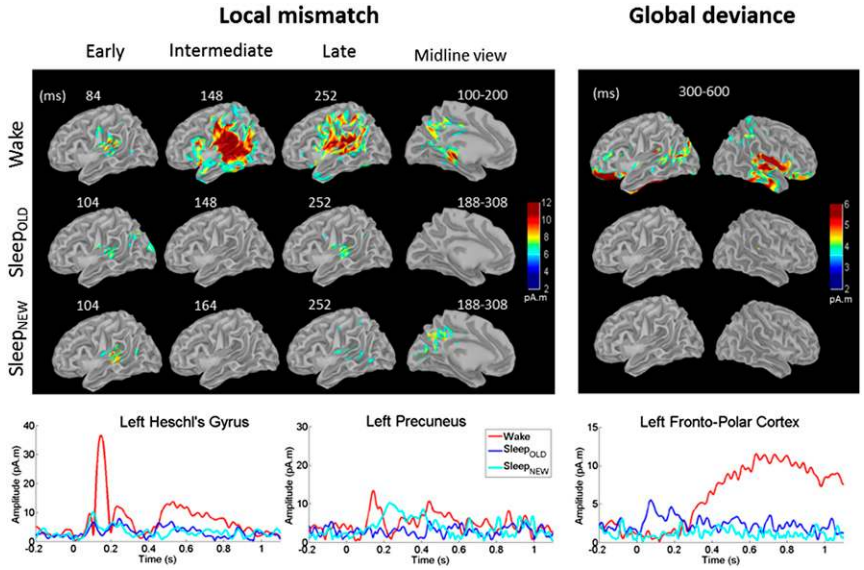

Fig. 4. Source reconstructions. Colors represent the intensity of estimated source currents in pA. Time series represent the time course of the absolute value of source current in specific regions of interest. (*Left*) Local mismatch. Auditory cortices respond with a slight delay during N2 sleep. Intermediate-latency activations vanish during sleep. A late effect is present during sleep, although attenuated in amplitude, and with delayed activation of the precuneus only for new stimuli. Time series are presented for the left Heschl gyrus and the precuneus. (*Right*) Global deviance. During wakefulness, broad parietal, frontal, and temporal activations are present. During sleep, this activity vanishes, except for an early transient activity for old stimuli heard previously during wakefulness, as seen on time series (N2-Sleep$_{OLD}$).

(Wake$_{PRE}$: 256–700 ms, $P < 10^{-4}$; Wake$_{POST}$: 136–680 ms, $P < 0.01$) with the characteristics of a classical P300 (Fig. S2). A comparison of Wake$_{PRE}$ and Wake$_{POST}$ revealed stronger sustained MEG activations in anterior areas during Wake$_{PRE}$ (596–672 ms, $P < 0.05$), despite similar amplitudes in auditory areas (Table S4). In N1 sleep, when subjects were still responding, the global effect continued to be elicited over temporal and anterior regions (N1-responsive: 176–700 ms, $P < 10^{-4}$); however, critically, even during N1 sleep, as soon as subjects ceased to be behaviorally responsive, the P300 vanished (N1-nonresponsive; Fig. 2*B*). In N2 sleep and REM sleep, subjects did not respond behaviorally to any global deviant, and no response to global deviance was seen. (ERPs and all MEG sensor results are presented in Fig. S2.) Note that in a recent study, Kouider et al. (39) detected markers of motor preparation (i.e., lateralized readiness potentials) in the descent to sleep, even in the absence of behavioral responses. In the present study, subjects made only unimanual responses, and thus we could not compute lateralized readiness potentials. Consequently, we cannot exclude the possibility of an automatic motor initiation during sleep, but can only conclude as to the absence of the P300 associated with the global effect.

Analyzing the old and new stimuli separately revealed an early and transient global effect to old stimuli over anterior sensors in N2 sleep (N2-Sleep$_{OLD}$: 48–188 ms, $P < 0.01$). No such activation was found for new stimuli introduced during sleep (N2-Sleep$_{NEW}$; Fig. 3*B*). A direct comparison of N2-Sleep$_{OLD}$ and N2-Sleep$_{NEW}$ stimuli revealed a significant interaction in the same anterior sensors (68–168 ms, $P < 0.05$). Note that during wakefulness, an early effect in those regions fell just short of significance (Wake$_{(PRE+POST)}$: 88–152 ms, $P = 0.05$).

In source reconstructions, the global effect during Wake comprised a first set of activations localized mainly to auditory areas (maximum at 144 ms in right superior temporal gyrus/planum temporale; MNI: 32.46 −26.02 10.34), associated with activations in bilateral precuneus, parahippocampal gyri, and posterior cingulate. This was followed by large and sustained activations in associative cortices (temporal and parietal lobes, right insula, posterior and superior cingulate cortices, dorsolateral prefrontal and lateral orbitofrontal cortices; Fig. 4, *Right*). No such activation was found during sleep; however, in N2-Sleep$_{OLD}$, an early and transient activity was found in frontoorbital areas, followed by small activations of the right supramarginal gyrus (140–340 ms).

In multivariate classification, the global effect was successfully decoded during Wake$_{PRE}$, with almost complete generalization to Wake$_{POST}$ (Fig. 5*A*, *Right*). Note that the effect was just above chance even before the onset of the fifth sound, an effect observed in previous work (34) and linked to the anticipation of global deviant sequences, given that the probability of their occurrence increases with the successive presentation of global standards. None of these effects generalized to sleep data (Fig. 5*A*). Testing the generalization from Wake$_{PRE}$ to N2-Sleep$_{(OLD+NEW)}$ revealed only a very transient generalization from 212 to 228 ms (Fig. 5*A*, *Right*). This effect was related to a transient period of generalization (196–252 ms, $P < 0.05$) for N2-Sleep$_{OLD}$ stimuli only (Fig. 5*B*, *Right*). No generalization was possible from Wake$_{PRE}$ to N2-Sleep$_{NEW}$ stimuli. Even when trained and tested specifically on the Sleep$_{(OLD+NEW)}$ dataset, the classifier was unable to correctly classify global deviant vs. global standard sequences (Fig. 5*C*, *Right*). These results suggest that during sleep, the brain is not responsive to global regularities, except for a transient period unique to previously learned stimuli.

Modulation of Evoked Responses Across Vigilance States. Beyond the evoked responses to auditory novelty, our paradigm also provide basic data on the evolution of auditory responses evoked by the first four sounds across the different states of vigilance. A clear dissociation was seen as a function of the latency of auditory responses (Fig. 2). The amplitude of the first measurable response to sound onset (first peak in Fig. 2*C*) remained unchanged across sleep stages (complete statistics in Table S5), although its latency increased significantly (Wake: 73.4 ms; N1-Sleep: 81.5 ms; N2-Sleep: 100.4 ms; REM: 94.2 ms); however the next peak (second peak in Fig. 2*C*) was dramatically reduced in amplitude during N1, N2, and REM sleep, and its latency was also increased (Wake: 158.2 ms; N1: 176 ms; N2: 179.8 ms; REM: 183.6 ms) (Table S6).

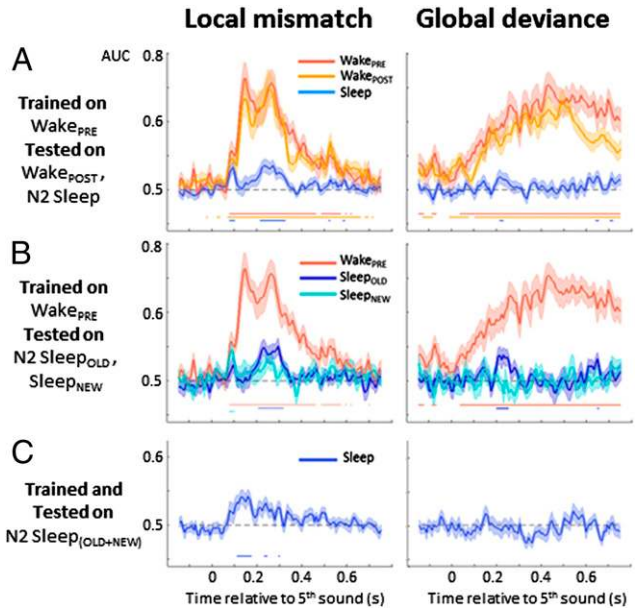

Fig. 5. Decoding the brain's novelty responses to local mismatch and to global deviance during wakefulness and N2 sleep. At each time point, multivariate classifiers were trained to discriminate either local standards from local deviants (aaaaa vs. aaaaB series, left column) or global standards from global deviants (frequent vs. rare series, right column). Each curve represents the AUC, a parameter-free measure of decoding success (chance level, 0.5). Significant decoding ($P < 0.05$) is indicated by a horizontal line. (*A*) Generalization from wake to sleep. A classifier was trained on the Wake$_{PRE}$ session and its ability to accurately classify local (*Left*) and global (*Right*) effects was tested on the same session (red), on Wake$_{POST}$ (orange) and on N2-Sleep$_{(OLD+NEW)}$ (blue). (*B*) Improved generalization for stimuli previously heard during wakefulness. A classifier was trained on Wake$_{PRE}$ and tested separately on Sleep$_{OLD}$ (dark blue) and Sleep$_{NEW}$ (cyan). (*C*) Decoders trained during sleep. A classifier was trained and tested on the N2-Sleep$_{(OLD+NEW)}$ dataset.

Because of the similarities in temporal profile and topography of this second peak and the local MMR, and because both components decreased during sleep, we examined whether these two phenomena were related across subjects. Regression analysis indeed revealed a positive correlation between the amplitudes of this second peak and of the intermediate MMR during N2 sleep ($r = 0.53$; $P < 0.05$), indicating that the reductions in the second auditory peak and the MMR are related phenomena.

After the second sound, it became harder to separate the peaks evoked by individual stimuli, but the overall envelope of responses was also strongly diminished during sleep (Fig. 2). In the local-global paradigm with awake and conscious subjects, a progressive ramping-up of brain responses across the four sounds has been described and tentatively ascribed to an expectation of the final sound (40). We verified that this ramping-up was present in our data during wakefulness (cluster analysis for slope different from 0, $P < 0.001$ in temporal areas), and that it diminished during N1 sleep and then N2 sleep (Table S7) while remaining significant (significant slope in N2 sleep, $P < 0.001$). A slight rebound was observed during REM sleep, with an effect size indistinguishable from that for N1 sleep.

Separate Assessment of Predictive Coding and Sensory Adaptation. Experiment 1 yielded a clear-cut vanishing of the global effect during sleep, but the results for the MMR were more ambiguous; a significant difference continued to be observed between local deviants and local standards, yet the main peak of the MMR decreased during N1 sleep and vanished during N2 and REM sleep. Given that this main peak has been associated with prediction error in previous studies (24–26), one hypothesis is that sleep selectively disrupts predictive coding and preserves only sensory adaptation. To evaluate this possibility, we ran a second experiment in which sensory adaptation and predictive coding were manipulated independently (Fig. 6). We replicated the aaaaa blocks, where rare "aaaaB" deviant sequences violate both prediction and adaptation. We also introduced novel blocks using aBaBa and aBaBB sequences, in which the dominant expectation is an alternation of the two sounds. Here predictive coding should induce a prediction error response to the final unexpected sound repetition in aBaBB, whereas passive adaptation makes the opposite prediction of a reduced activation to repetition (or no effect at all if a single stimulus repetition fails to yield a significant adaptation).

The results for the aaaaa blocks fully replicated our earlier observations. During wakefulness, deviant sequences elicited an MMR with virtually the same three-component shape as in the first experiment (Fig. 6*A*). Again, an intermediate MMR effect was clearly present during wakefulness (108–156 ms in temporal areas, $P < 0.05$) but vanished during N2 sleep, leaving only the

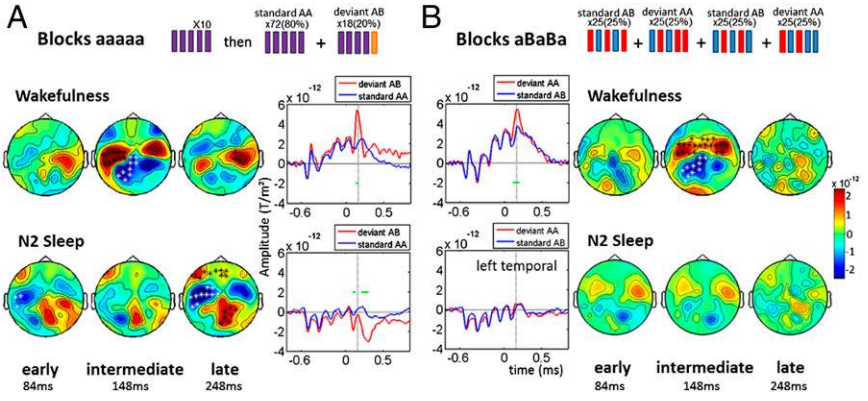

Fig. 6. Dissociation between disrupted predictive coding and preserved sensory adaptation during sleep. (*A*) Block aaaaa: replication of experiment 1. During wakefulness, aaaaB deviants that violate both prediction and adaptation elicited an MMR with three components (early, intermediate, and late). During N2 sleep, early and late components remained present, but the intermediate component vanished. (*B*) Block aBaBa: dissociation of prediction and adaptation. During wakefulness, the aBaBB deviants that violate prediction but not adaptation elicited an MMR only during the intermediate time periody. During N2 sleep, no significant difference remained. Topographies for each components are shown, with significant clusters (*$P < 0.05$). aERF time series with significant activations for the left temporal MEG sensor are displayed (horizontal green lines). The vertical dotted line indicates the peak of the intermediate effect (148 ms after the deviant sound).

early and late effects (early, 84–124 ms, $P < 0.05$; late, 204–300 ms, $P < 0.01$). Crucially, the aBaBa blocks revealed that this intermediate peak was entirely imputable to prediction error. During wakefulness, the deviant series aBaBB elicited an MMR characterized by a single deflection peaking at around 150 ms (100–200 ms, $P = 0.001$) and essentially identical in latency and topography to the intermediate effect in aaaaa blocks (Fig. 6*B*). This effect vanished during N2 sleep, such that the difference between aBaBa and aBaBB failed to reach significance. Thus, in a paradigm that separates predictive coding from sensory adaptation, sleep appears to selectively disrupt predictive coding.

Discussion

We investigated whether predictive coding, which is considered a fundamental property of the cortex, continues to operate during sleep. To this end, we tracked the responses of the sleeping brain when presented with auditory novelties at two distinct levels of complexity, local (single-vowel change) and global (whole-sequence change), using a paradigm previously demonstrated to engage predictive coding mechanisms (25). Despite the continued presence of strong auditory potentials during sleep, the global effect (P300) disappeared abruptly, simultaneous with the loss of behavioral responsiveness during the descent to sleep, and was absent in both NREM and REM sleep. Local violations continued to elicit a distinctive response, but the peak of this local MMR, at around 150 ms, was sharply reduced. We then investigated which mechanism accounted for the residual mismatch effect that remained present during sleep. By dissociating predictive coding from sensory adaptation, we demonstrated that the mismatch peak that vanished during sleep was specifically associated with a prediction error signal. We now discuss how these results clarify whether and how sleep disrupts the processing of novel external stimuli.

Preserved Auditory Processing During Sleep. Our results firmly establish that auditory stimuli (here single vowels) continue to enter the cortex and to be discriminated during sleep. Early perceptual responses of unchanged amplitude were detected in auditory cortices across all states of vigilance (Figs. 2 and 4). These early activations in primary auditory areas are in line with other studies demonstrating activation of auditory cortices during sleep (6, 7, 9, 10, 12). Animal studies suggest that the burst firing mode of the thalamus during sleep, with its alternating on and off states, may be as effective as the tonic mode characteristic of wakefulness in relaying incoming sensory information to the cortex (41). However, changes in neuromodulatory control of thalamocortical excitability during sleep may attenuate sensory precision (42), which in turn would reduce the rate of evidence accumulation in sensory areas, thereby explaining the progressive increase in auditory latencies during sleep observed in the present study and previous studies (43, 44). This attenuation of the precision of sensory prediction errors also may explain the subsequent disruption in global and local effects (42).

Disrupted Predictive Coding During Sleep. Previous research with inattentive subjects as well as patients in coma and vegetative states has established that the global novelty response, associated with a P300 on EEG, depends on a conscious appraisal of the auditory sequence (19, 33, 35). Our present findings extend this result to sleep, demonstrating that the brain response to global novelty vanished abruptly with the loss of responsiveness during sleep. The all-or-none disappearance of the P300 occurred as early as stage 1 sleep, in which subjects were fluctuating between responsive and nonresponsive states; responsive subjects exhibited a significant global effect on MEG and a P300 wave on EEG, whereas nonresponsive subjects no longer did. This disappearance cannot be ascribed solely to a lack of motor preparation, considering that in both the present work (Fig. S4) and previous research (25), the global effect remained present with virtually identical topography, temporal profile, and source localization when awake subjects were told merely to attend to the stimuli without overtly responding.

Our present results reinforce the notion that the global novelty response and, more generally, the P300 wave are phenomena that reflect conscious processes (19, 33, 35, 45, 46) and that vanish suddenly under nonconscious conditions (17). Our results depict stage N1 sleep as a transition process from wakefulness to sleep, characterized by a mixture of conscious and nonconscious states inside the alpha-suppression periods. This hypothesis may explain previous results showing an attenuated P300 during N1 sleep (44); this result would arise from averaging over these two states, which indeed would have remained indistinguishable had we not used an explicit behavioral task.

Our findings are partially at odds with a set of previous studies using the oddball paradigm that reported a small late posterior positivity during sleep at around 300 ms (47–50) or 450 ms (44, 51) after deviant sounds. We note, however, that the oddball paradigm, unlike our present local-global paradigm, fails to dissociate the successive stages of novelty detection that are now known to have very different properties in relation to consciousness (19, 25, 33, 34). Thus, we cannot exclude the possibility that those previous studies observed only the delayed response to a low-level (local) violation, rather than a genuine P300 response to high-level conscious predictive coding. Another possibility is that the stimuli used in these previous studies induced short periods of awakening. Here we purposely used low-intensity sounds (46 dB) and carefully monitored sleep stages to avoid this difficulty. Furthermore, we searched for novelty responses using a sensitive technique of MEG recording with 306 sensors followed by multivariate decoding, trained either directly on sleep data (Fig. 5*C*) or on a more extensive set of wake data from the same subject and then tested for generalization to sleep (Fig. 5*A*). Because none of these efforts revealed a global novelty response, we can be confident that this response disappears during sleep in our paradigm.

The only exception was a small, early (<300 ms), and transient global effect that remained elicited only by deviant sequences that had been previously heard consciously during wakefulness (Fig. 3*B*). This result suggests that although the sleeping brain is unable to acquire a novel sequence during sleep, it remains able to detect deviations from a highly overlearned sequence heard repeatedly before sleep. The early time window of this effect, along with the weak and transient generalization of decoding from presleep to sleep (Fig. 5*B*), suggest that this response does not result from the sustained activation of the distributed "global workspace" underlying conscious responses to novelty (17, 19), but rather may arise from a modular and automatic process localized to frontopolar and periauditory areas (Fig. 4). On repetition during wakefulness, a sequence of five vowels (e.g., a, a, a, a, u) may become so highly familiar so as to be stored as a unified auditory template similar to a word. The difference in brain response when a rare sequence is presented (e.g., a, a, a, a, a) may then reflect a sensory adaptation effect in units coding for this level (29). At any rate, the absence of any global effect with unfamiliar stimuli imply that such storage of frequent "words," if present, is disrupted during sleep.

Disrupted MMR but Preserved Adaptation During Sleep. Previous research using the local-global paradigm has indicated that, contrary to the global response, the local MMR can be preserved under conditions of distraction or unconsciousness (19, 33). Thus, we expected that this response might remain present during sleep. This prediction was only partially upheld, because a specific part of the MMR elicited by local vowel deviants was also strongly affected by sleep. During wakefulness, the MMR was characterized by three steps of auditory processing: an early effect before

100 ms, an intermediate effect peaking around 150 ms (the MMN on EEG), and a late effect after 240 ms. During sleep, the intermediate MMR effect/MMN was specifically reduced during N1 sleep and ultimately dropped to an undetectable level in N2 and REM sleep (Fig. 2*A*). Experiment 2 replicated these results (Fig. 6*A*) and demonstrated that the intermediate MMR component was specifically elicited by prediction errors during wakefulness, an effect that completely disappeared during sleep (Fig. 6*B*). Thus, the MMR observed during wakefulness can be decomposed into (*i*) early and late components that result from adaptation mechanisms and remain during sleep, and (*ii*) a sharp intermediate peak that results from a prediction error and vanishes during sleep. This decomposition of the MMR is consistent with previous studies describing it as a complex phenomenon arising from multiple cortical areas with different qualitative properties (22, 52, 53) and associating the intermediate MMR peak with predictive coding (24–26).

The formation of a prediction error signal is thought to require a bidirectional transfer of information in both bottom-up and top-down directions, either locally across cortical layers (26) or across multiple areas of the cortical hierarchy (18). Previous evidence suggests that the generators of the MMN extend beyond primary auditory cortices and involve a broad network including frontal and opercular cortices (14, 22, 54). Our source reconstructions confirm these localizations and suggest that they are specific to the intermediate time window of the MMR. The left inferior frontal pars opercularis area (Broca's area) location is also coherent with our use of vowel sequences, because this region is involved in the representation of structured language sequences (55).

Multivariate classifiers trained at the time of the intermediate mismatch peak were able to decode local deviants during wakefulness, but failed to generalize either to sleep (Fig. 5) or to other time periods (see the full temporal generalization matrix in Fig. S3). In previous work, the temporal generalization of a classifier from one time point to another has been shown to provide detailed information on the time course of brain activation (37). King et al. (38) applied this method to the local-global paradigm and showed, exactly as in the present work, that the intermediate MMR was focal in time and did not generalize to the early and late time periods.

Despite the disruption of markers of predictive coding during both NREM and REM sleep, a slight recovery of the progressive ramping-up of brain responses was observed during REM sleep (Fig. 2). This effect has been previously associated with an expectation of the fifth sound in the sequence (40), an interpretation that would appear to contradict the observed disruption of predictions during sleep. However, this ramping-up also can be interpreted as a passive summation of the activation evoked by each successive vowel, without involving top-down expectations. Further research is needed to disentangle these two interpretations, and to clarify which aspects of the processing of external auditory stimuli may recover during REM sleep.

Unlike predictive coding, adaptation is considered a basic property of bottom-up sensory transmission localized to the primary auditory cortex (23, 28, 56). We indeed showed that the early MMR effect localizes almost exclusively to auditory areas during both wakefulness and sleep (Fig. 4). The late effect was also localized to auditory cortices during sleep, but activations propagated more broadly into the cortex during wakefulness (Fig. 4). The similarities of the mechanisms in early and late MMR are strengthened by the successful temporal generalization from one effect to the other in both states of vigilance (Fig. S3). Decoding analyses also confirmed the similarities of these effects between wakefulness and sleep, because decoding generalized successfully from one state to the other (Fig. 5*A* and Fig. S3).

The hypothesis of preserved sensory adaptation during sleep has been supported by a recent electrophysiological study in rats (9). Our results confirm this possibility in humans. They further show that the recovery from adaptation for deviant sounds is particularly large for stimuli that were never heard before sleep (Fig. 3), compared with sounds that were extensively presented before sleep and while falling asleep. Only the new local deviants elicited activations spreading into the precuneus (Fig. 4). By reaching this region putatively involved in consciousness and self-awareness (57), novel deviant tones may bring the brain closer to the awakening threshold. Thus, the proposed preservation of stimulus-specific adaptation during sleep may explain why the presentation of novel sounds may lead to awakening, whereas familiar sounds (e.g., ticking clock) do not.

Overall, our results indicate that the cortex continues to process auditory stimuli during sleep, and to adapt to them, but that two components of brain activity related to hierarchical predictive coding—the global effect and the intermediate peak of the local MMR—vanish during sleep. Future research should test whether these findings can be generalized to other prediction paradigms that are also thought to depend on a bidirectional bottom-up and top-down exchange of cortical signals (18). This hypothesis would be compatible with the vast literature that indicates a breakdown of cortical communication and temporal integration during sleep (3–5).

Materials and Methods

Human brain signals were recorded with combined MEG/EEG during wakefulness and sleep. On the previous night, sleep was restricted to 4 h between 3:00 and 7:00 AM. Sleep restriction was controlled by an actimeter (Actiwatch 7, Sleepwatch software 7.5; CamNtech) worn on the nondominant wrist during the 48 h before the experiment and measuring motor activity. The EEG-MEG experiment lasted a maximum of 3 h and was followed by anatomic MRI. The main steps of methods are presented here; more detailed information is provided in *SI Materials and Methods*.

Experiment 1.

Auditory stimuli and block design. Stimuli consisted of four pairs of phonetically distant French vowels (100-ms duration). In each block of stimuli, one pair was used to prepare 100 sequences of five vowels each (150-ms stimulus onset asynchrony between vowels). Sequences were separated by silent gaps of variable duration (700–1,000 ms intertrial interval, 50-ms steps). The vowels in each sequence were either all identical ("local standard," denoted aaaaa) or with a different fifth vowel ("local deviant," denoted aaaaB). Two types of blocks were presented. In aaaaa blocks, the most frequent sequence, the "global standard," was aaaaa (presented 10 times during an initial habituation phase, then 80% of the time), and the sequence aaaaB was presented as a rare "global deviant" (20% of trials). In aaaaB blocks, the roles were inverted, as described previously (19, 25). Each type of block used a different vowel pair (one pair for aaaaa blocks, another pair for aaaaB blocks) and was repeated twice to counterbalance the vowels used as sounds a and B.
Procedure. Auditory sequences were presented in short blocks before ($Wake_{PRE}$), during (sleep), and immediately after ($Wake_{POST}$) a morning nap. During wakefulness, subjects were asked to click a button after each global deviant on half of the blocks (one aaaaa block and one aaaaB block), and to remain passive but attentive on the other half. This procedure was adopted to document the global effect with and without associated motor response; because no major differences were observed between those two conditions (see Fig. S4), they were combined for analysis. During the sleep session, subjects fell asleep while hearing the stimuli. To monitor awareness, they were asked to respond whenever they were aware of global deviants. During NREM sleep stage 1 (N1-Sleep), occasional responses were still emitted, allowing us to retrospectively split the data into N1-responsive and N1-nonresponsive states. Once subjects reached NREM sleep stage 2 (N2-Sleep), as indicated by online EEG monitoring, blocks with previously presented auditory stimuli (stimulus set 1, termed $N2\text{-}Sleep_{OLD}$ blocks) were randomly presented with new blocks using vowels never heard during wakefulness (stimulus set 2, termed $N2\text{-}Sleep_{NEW}$ blocks) but sharing the same local and global regularity structure as the old blocks. Thus, we evaluated whether the local and global novelty responses could be acquired as well as expressed during sleep. The order of presentation of $Sleep_{OLD}$ and $Sleep_{NEW}$ blocks was fully randomized. Only stimulus set 2 blocks were presented during $Wake_{POST}$.
Subjects. Thirty-one healthy, right-handed subjects, age 18–35 y and evaluated as good sleepers, were recruited on a voluntary basis after giving written informed consent. This study was approved by the Ethical Committee Ile de

France VII (Comité de Protection des Personnes 08-021). Only subjects who managed to sleep during the MEG and with a sufficient number of trials and signal-to-noise levels to identify auditory ERFs (aERF) were retained for analysis (for N2-Sleep: $n = 23$ subjects reached this stage/$n = 19$ subjects showed aERFs; N2-Sleep$_{OLD}$: $n = 23/18$; N2-Sleep$_{NEW}$: $n = 23/18$; REM sleep: $n = 11/9$). During N1 sleep, subject inclusion was also based on compliance with the motor task (aERF: $n = 16$; good compliance: $n = 13$).

Simultaneous MEG/EEG recording. MEG and EEG signals were recorded simultaneously with the Elekta Neuromag system with the subject in the supine position (204 planar gradiometers and 102 magnetometers) and the built-in EEG system (60 channels). An electrocardiogram (ECG), electro-oculogram (EOG) (horizontal and vertical), and chin electromyogram (EMG) were recorded as auxiliary bipolar channels. EEG, EOG, and EMG signals were used to monitor sleep stages online. The head position in the MEG sensor array was acquired continuously during each block through four head-position indicator coils attached to the scalp and previously digitized with respect to three anatomic landmarks (nasion and preauricular points; Polhemus Isotrak system).

Sleep analysis. The sleep stages were rescored off-line by two independent sleep experts (M.S. and M.E.) according to the 2007 AASM guidelines (FASST software; www.montefiore.ulg.ac.be/~phillips/FASST.html). Interscorer agreement was high (96%). Scorers jointly agreed on the remaining recordings, and any ambiguous period or transition between two stages was removed from analysis. For N1 sleep analysis, only periods with alpha suppression were retained. In N2 sleep, K-complexes and microarousals were manually detected and excluded from the analysis. An example of sleep scoring is shown in Fig. S5.

Preprocessing and data analysis. Data were preprocessed applying successively signal space separation correction, continuous head movement compensation, and MEG bad channel correction (MaxFilter; Elekta Neuromag), downsampling (250 Hz) and filtering (0.3–30 Hz) (MNE; martinos.org/mne/stable/index.html), epoching (−200 to 1,450 ms after sequence start), EEG bad channel interpolation and average referencing (Fieldtrip; www.ru.nl/neuroimaging/fieldtrip), and outlier trials rejection (audition.ens.fr/adc/NoiseTools/). Statistical analyses were performed with cluster permutation tests corrected for multiple comparisons over time and sensor space for each type of sensors (Fieldtrip; Monte Carlo method, 1,000 permutations). Based on previous results (19, 25), search windows were defined between 48 and 498 ms for the local mismatch effect and between 48 and 700 ms for the global effect for both EEG and MEG data. For simplicity, we report topographies, time series, and statistical analyses conducted on MEG sensors oriented on the *d-y* axis (two gradiometers); results were replicated in the other sensors and at the source level. Further explanations and additional results are provided in Figs. S1 and S2. MEG time series for local and global effects are displayed for a sensor lying next to the auditory cortex, selected based on previous MEG studies (19, 25) and lateralized to the left hemisphere given our use of linguistic stimuli (vowels).

Amplitudes and latencies of early auditory responses and local and global effects across states of vigilance were further analyzed on a set of four gradiometers lying closest to the left auditory cortex. Analyses of the slope of evoked responses along sequences were performed by computing the linear regression between the first and fifth sounds and comparing slopes between stages of vigilance. Because the number of subjects differed among sleep stages, we tested for differences using the paired Wilcoxon signed-rank test, using only those subjects for whom data were available in the two vigilance states tested (Tables S1, S2, S3, S4, S5, S6, and S7).

Source reconstructions. Anatomic T1-weighted MRI images were acquired for each subject (3-T; Siemens TRIO). Cortex segmentation (gray-white matter boundary) was done with Freesurfer (surfer.nmr.mgh.harvard.edu/). Estimation of current source density was performed with BrainStorm (neuroimage.usc.edu/brainstorm/). After cortical and scalp reconstructions, anatomy and MEG signals were coregistered using head position indicators and EEG electrode positions on the scalp previously digitized. The forward problem was computed using an overlapping spheres model. Noise covariance was estimated from empty-room MEG recordings acquired before each subject's recording. Individual sources were computed with weighted minimum-norm method and dSPM option (depth weighting factor of 0.8, loosing factor of 0.2 for dipole orientation), separately for local and global effects. They were then projected on a standard anatomic template before averaging across subjects. Absolute values of the time series in regions of interest are shown.

Multivariate decoding. Multivariate classifiers were trained on single-trial sensor-level data as described previously (34). Decoding performance was summarized with an empirical receiver operating characteristic (ROC) analysis and its AUC. AUCs were computed for each subject, then averaged across subjects. Significance was tested within subjects using the Mann–Whitney *U* test across trials. Correspondingly, across-subjects statistics were computed using the Wilcoxon signed-rank test on the mean predicted probability of the true trial class. Using the Wake$_{PRE}$ data in a [−150, 750]-ms time window, two classifiers were trained separately for the local effect (separating local deviants from local standards) and for the global effect (separating global deviants from global standards). These classifiers were subsequently tested on their ability to generalize, on a single-trial basis, to N2-Sleep and to Wake$_{POST}$. To maximize the detection of novelty effects during sleep, two additional classifiers were trained only on N2-Sleep data.

Experiment 2. The design was identical to experiment 1 with the following exceptions (Fig. 6). Two blocks of 100 sequences were presented: aaaaa blocks identical to the first experiment and a second type of block in which new vowel pairs were used to build two standard sequences of five alternating vowels (aBaBa and BaBaB) and two deviant sequences including a final repetition (aBaBB and BaBaa). Sequences were presented at random with an equal frequency (25% each). In this manner, the two vowels had the same absolute frequency but the transition probabilities differed, because vowel alternation was much more probable (7/8) than vowel repetition (1/8).

Eleven healthy, right-handed subjects, age 18–35 y, different from those in the first experiment, were recruited. Because the focus was on the MMR, subjects were not asked to perform any explicit behavioral task. All subjects fell asleep and were included in the analysis. Statistical cluster permutation tests were computed between 0 and 300 ms after the fifth sound of series, a search window defined from the results of the first experiment to focus on the three MMR components.

ACKNOWLEDGMENTS. We are grateful to Bernadette Martins and the Neurospin staff for administrative support and to nurses Laurence Laurier, Véronique Joly-Testault, and Gaëlle Mediouni for their help in recruitment and data acquisition. We thank Laurent Cohen and Claire Sergent for recording the stimuli; Anne Kösem, Lucie Charles, Catherine Wacongne, Sebastien Marti, and Rafik Keffache for their help piloting the study and useful comments; and Laurent Cohen and Hélène Bastuji for useful discussions. We gratefully acknowledge Alain de Cheveigné's help in denoising data and Jean-Didier Lemaréchal's help in developing the MEG preprocessing software. This work was supported by grants from Institut National de la Santé et de la Recherche Médicale (INSERM) and Journées de Neurologie de Langue Française (to M.S.); INSERM, Commissariat à l'Energie Atomique (CEA), Fondation Roger de Spoelberch, and European Research Council (Senior Grant "NeuroConsc") (to S.D.); Direction Générale de l'Armement (to J.-R.K.); and Stic-Amsud "RTBRAIN" (to J.D.S.). The Neurospin MEG facility is sponsored by grants from INSERM, CEA, Fondation pour la Recherche Médicale, the Bettencourt-Schueller Foundation, and the Région île-de-France.

1. Rechtschaffen A, Hauri P, Zeitlin M (1966) Auditory awakening thresholds in REM and NREM sleep stages. *Percept Mot Skills* 22(3):927–942.
2. Steriade M, McCormick DA, Sejnowski TJ (1993) Thalamocortical oscillations in the sleeping and aroused brain. *Science* 262(5134):679–685.
3. Massimini M, et al. (2005) Breakdown of cortical effective connectivity during sleep. *Science* 309(5744):2228–2232.
4. Horovitz SG, et al. (2009) Decoupling of the brain's default mode network during deep sleep. *Proc Natl Acad Sci USA* 106(27):11376–11381.
5. Tagliazucchi E, et al. (2013) Breakdown of long-range temporal dependence in default mode and attention networks during deep sleep. *Proc Natl Acad Sci USA* 110(38):15419–15424.
6. Peña JL, Pérez-Perera L, Bouvier M, Velluti RA (1999) Sleep and wakefulness modulation of the neuronal firing in the auditory cortex of the guinea pig. *Brain Res* 816(2): 463–470.
7. Edeline J-M, Dutrieux G, Manunta Y, Hennevin E (2001) Diversity of receptive field changes in auditory cortex during natural sleep. *Eur J Neurosci* 14(11):1865–1880.
8. Issa EB, Wang X (2008) Sensory responses during sleep in primate primary and secondary auditory cortex. *J Neurosci* 28(53):14467–14480.
9. Nir Y, Vyazovskiy VV, Cirelli C, Banks MI, Tononi G (2013) Auditory responses and stimulus-specific adaptation in rat auditory cortex are preserved across NREM and REM sleep. *Cereb Cortex*, 10.1093/cercor/bht328.
10. Portas CM, et al. (2000) Auditory processing across the sleep-wake cycle: Simultaneous EEG and fMRI monitoring in humans. *Neuron* 28(3):991–999.
11. Czisch M, et al. (2002) Altered processing of acoustic stimuli during sleep: Reduced auditory activation and visual deactivation detected by a combined fMRI/EEG study. *Neuroimage* 16(1):251–258.
12. Dang-Vu TT, et al. (2011) Interplay between spontaneous and induced brain activity during human non-rapid eye movement sleep. *Proc Natl Acad Sci USA* 108(37): 15438–15443.
13. Bastuji H, Perrin F, Garcia-Larrea L (2002) Semantic analysis of auditory input during sleep: Studies with event-related potentials. *Int J Psychophysiol* 46(3): 243–255.

14. Näätänen R, Paavilainen P, Rinne T, Alho K (2007) The mismatch negativity (MMN) in basic research of central auditory processing: A review. *Clin Neurophysiol* 118(12): 2544–2590.
15. Näätänen R, Tervaniemi M, Sussman E, Paavilainen P, Winkler I (2001) "Primitive intelligence" in the auditory cortex. *Trends Neurosci* 24(5):283–288.
16. Sutton S, Braren M, Zubin J, John ER (1965) Evoked-potential correlates of stimulus uncertainty. *Science* 150(3700):1187–1188.
17. Dehaene S, Changeux J-P (2011) Experimental and theoretical approaches to conscious processing. *Neuron* 70(2):200–227.
18. Friston K (2005) A theory of cortical responses. *Philos Trans R Soc Lond B Biol Sci* 360(1456):815–836.
19. Bekinschtein TA, et al. (2009) Neural signature of the conscious processing of auditory regularities. *Proc Natl Acad Sci USA* 106(5):1672–1677.
20. Plourde G, Picton TW (1991) Long-latency auditory evoked potentials during general anesthesia: N1 and P3 components. *Anesth Analg* 72(3):342–350.
21. Koelsch S, Heinke W, Sammler D, Olthoff D (2006) Auditory processing during deep propofol sedation and recovery from unconsciousness. *Clin Neurophysiol* 117(8): 1746–1759.
22. Garrido MI, Kilner JM, Stephan KE, Friston KJ (2009) The mismatch negativity: A review of underlying mechanisms. *Clin Neurophysiol* 120(3):453–463.
23. Farley BJ, Quirk MC, Doherty JJ, Christian EP (2010) Stimulus-specific adaptation in auditory cortex is an NMDA-independent process distinct from the sensory novelty encoded by the mismatch negativity. *J Neurosci* 30(49):16475–16484.
24. Todorovic A, de Lange FP (2012) Repetition suppression and expectation suppression are dissociable in time in early auditory evoked fields. *J Neurosci* 32(39):13389–13395.
25. Wacongne C, et al. (2011) Evidence for a hierarchy of predictions and prediction errors in human cortex. *Proc Natl Acad Sci USA* 108(51):20754–20759.
26. Wacongne C, Changeux J-P, Dehaene S (2012) A neuronal model of predictive coding accounting for the mismatch negativity. *J Neurosci* 32(11):3665–3678.
27. Fiorillo CD (2008) Towards a general theory of neural computation based on prediction by single neurons. *PLoS ONE* 3(10):e3298.
28. Ulanovsky N, Las L, Nelken I (2003) Processing of low-probability sounds by cortical neurons. *Nat Neurosci* 6(4):391–398.
29. May PJC, Tiitinen H (2010) Mismatch negativity (MMN), the deviance-elicited auditory deflection, explained. *Psychophysiology* 47(1):66–122.
30. Atienza M, Cantero JL, Escera C (2001) Auditory information processing during human sleep as revealed by event-related brain potentials. *Clin Neurophysiol* 112(11): 2031–2045.
31. Cote KA (2002) Probing awareness during sleep with the auditory odd-ball paradigm. *Int J Psychophysiol* 46(3):227–241.
32. Ruby P, Caclin A, Boulet S, Delpuech C, Morlet D (2008) Odd sound processing in the sleeping brain. *J Cogn Neurosci* 20(2):296–311.
33. Faugeras F, et al. (2012) Event related potentials elicited by violations of auditory regularities in patients with impaired consciousness. *Neuropsychologia* 50(3):403–418.
34. King JR, et al. (2013) Single-trial decoding of auditory novelty responses facilitates the detection of residual consciousness. *Neuroimage* 83:726–738.
35. Sitt JD, et al. (2014) Large-scale screening of neural signatures of consciousness in patients in a vegetative or minimally conscious state. *Brain* 137(Pt 8):2258–2270.
36. Horváth J, Winkler I (2004) How the human auditory system treats repetition amongst change. *Neurosci Lett* 368(2):157–161.
37. King J-R, Dehaene S (2014) Characterizing the dynamics of mental representations: The temporal generalization method. *Trends Cogn Sci* 18(4):203–210.
38. King J-R, Gramfort A, Schurger A, Naccache L, Dehaene S (2014) Two distinct dynamic modes subtend the detection of unexpected sounds. *PLoS ONE* 9(1):e85791.
39. Kouider S, Andrillon T, Barbosa LS, Goupil L, Bekinschtein TA (2014) Inducing task-relevant responses to speech in the sleeping brain. *Curr Biol* 24(18):2208–2214.
40. Chennu S, et al. (2013) Expectation and attention in hierarchical auditory prediction. *J Neurosci* 33(27):11194–11205.
41. Sherman SM (2001) Tonic and burst firing: Dual modes of thalamocortical relay. *Trends Neurosci* 24(2):122–126.
42. Hobson JA, Friston KJ (2012) Waking and dreaming consciousness: Neurobiological and functional considerations. *Prog Neurobiol* 98(1):82–98.
43. Nordby H, Hugdahl K, Stickgold R, Bronnick KS, Hobson JA (1996) Event-related potentials (ERPs) to deviant auditory stimuli during sleep and waking. *Neuroreport* 7(5): 1082–1086.
44. Bastuji H, García-Larrea L, Franc C, Mauguière F (1995) Brain processing of stimulus deviance during slow-wave and paradoxical sleep: A study of human auditory evoked responses using the oddball paradigm. *J Clin Neurophysiol* 12(2):155–167.
45. Sergent C, Baillet S, Dehaene S (2005) Timing of the brain events underlying access to consciousness during the attentional blink. *Nat Neurosci* 8(10):1391–1400.
46. Del Cul A, Baillet S, Dehaene S (2007) Brain dynamics underlying the nonlinear threshold for access to consciousness. *PLoS Biol* 5(10):e260.
47. Niiyama Y, Fujiwara R, Satoh N, Hishikawa Y (1994) Endogenous components of event-related potential appearing during NREM stage 1 and REM sleep in man. *Int J Psychophysiol* 17(2):165–174.
48. Cote KA, Campbell KB (1999) P300 to high intensity stimuli during REM sleep. *Clin Neurophysiol* 110(8):1345–1350.
49. Cote KA, Etienne L, Campbell KB (2001) Neurophysiological evidence for the detection of external stimuli during sleep. *Sleep* 24(7):791–803.
50. Takahara M, Nittono H, Hori T (2006) Effect of voluntary attention on auditory processing during REM sleep. *Sleep* 29(7):975–982.
51. Sallinen M, Kaartinen J, Lyytinen H (1996) Processing of auditory stimuli during tonic and phasic periods of REM sleep as revealed by event-related brain potentials. *J Sleep Res* 5(4):220–228.
52. Giard MH, et al. (1995) Separate representation of stimulus frequency, intensity, and duration in auditory sensory memory: An event-related potential and dipole-model analysis. *J Cogn Neurosci* 7(2):133–143.
53. Pegado F, et al. (2010) Probing the lifetimes of auditory novelty detection processes. *Neuropsychologia* 48(10):3145–3154.
54. Opitz B, Rinne T, Mecklinger A, von Cramon DY, Schröger E (2002) Differential contribution of frontal and temporal cortices to auditory change detection: fMRI and ERP results. *Neuroimage* 15(1):167–174.
55. Petersson KM, Hagoort P (2012) The neurobiology of syntax: Beyond string sets. *Philos Trans R Soc Lond B Biol Sci* 367(1598):1971–1983.
56. Fishman YI, Steinschneider M (2012) Searching for the mismatch negativity in primary auditory cortex of the awake monkey: Deviance detection or stimulus specific adaptation? *J Neurosci* 32(45):15747–15758.
57. Cavanna AE, Trimble MR (2006) The precuneus: A review of its functional anatomy and behavioural correlates. *Brain* 129(Pt 3):564–583.